

AD-A082 214

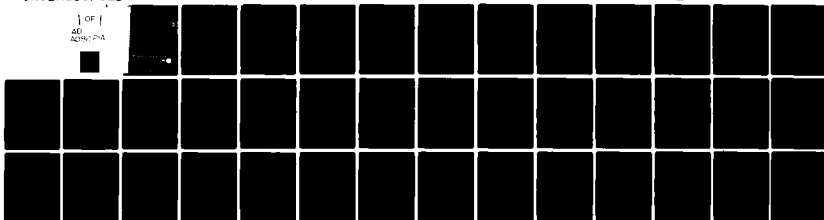
GEORGIA INST OF TECH ATLANTA SCHOOL OF ELECTRICAL EN--ETC F/6 20/14  
PARAMETRIC INVESTIGATION OF RADOME ANALYSIS METHODS.(U)  
FEB 80 G K HUDDLESTON H L BASSETT AFOSR-77-3469

UNCLASSIFIED

AFOSR-TR-80-0218

NL

1 OF 1  
AD  
A082 214



END  
DATE  
FILMED  
4-80  
DTIC

**AFOSR-TR- 80 - 0218**

**PARAMETRIC INVESTIGATION  
OF  
RADOME ANALYSIS METHODS**

**AD A082214**

**LEVEL**

**OPTIC  
ECTE  
MAR 24 1980**

**By**

**G. K. Huddleston, H. L. Bassett, & J. M. Newton**

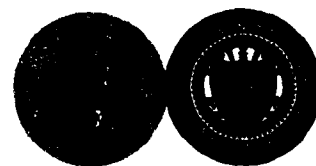
**Prepared for**

**AIR FORCE OFFICE OF SCIENTIFIC RESEARCH (AFSC)  
BOLLING AIR FORCE BASE, D. C. 20332**

**ANNUAL TECHNICAL REPORT  
GRANT AFOSR-77-3469  
1 October 1978 - 30 September 1979**

**February 1980**

**GEORGIA INSTITUTE OF TECHNOLOGY  
SCHOOL OF ELECTRICAL ENGINEERING  
ATLANTA, GEORGIA 30332**



**Approved for public release;  
distribution unlimited.**

**80 3 20 030**

**DC FILE COPY**

UNCLASSIFIED

SECURITY CLASSIFICATION OF THIS PAGE (When Data Entered)

1. REPORT DOCUMENTATION PAGE		READ INSTRUCTIONS BEFORE COMPLETING FORM	
1. REPORT NUMBER <b>AFOSR TR-80-0218</b>	2. GOVT ACCESSION NO.	3. RECIPIENT'S CATALOG NUMBER	
4. TITLE (and Subtitle) Parametric Investigation of Radome Analysis Methods	5. TYPE OF REPORT & PERIOD COVERED Annual Technical Report October 1, 1978-Sept. 30, 1979		
7. AUTHOR(s) G. K. Huddleston, H. L. Bassett, and J. M. Newton	6. PERFORMING ORG. REPORT NUMBER		
9. PERFORMING ORGANIZATION NAME AND ADDRESS Georgia Institute of Technology School of Electrical Engineering Atlanta, Georgia 30332	8. CONTRACT OR GRANT NUMBER(s) AFOSR-77-3469		
11. CONTROLLING OFFICE NAME AND ADDRESS Air Force Office of Scientific Research /NP Directorate of Physics Bolling Air Force Base, D.C. 20332	10. PROGRAM ELEMENT, PROJECT, TASK AREA & WORK UNIT NUMBERS 61102F / 2301 / A6 16 17		
14. MONITORING AGENCY NAME & ADDRESS (if different from Controlling Office) 1-411	12. REPORT DATE Feb 1980		
	13. NUMBER OF PAGES 35		
	15. SECURITY CLASS. (of this report) Unclassified		
16. DISTRIBUTION STATEMENT (of this Report) Approved for public release; distribution unlimited.			
17. DISTRIBUTION STATEMENT (of abstract entered in Block 20, if different from Report) 1-411-78-3469-21			
18. SUPPLEMENTARY NOTES			
19. KEY WORDS (Continue on reverse side if necessary and identify by block number) Radome Analysis Millimeter Wave Radomes Monopulse Antenna Synthesis			
20. ABSTRACT (Continue on reverse side if necessary and identify by block number) The status is described of a research program whose objective is to determine the accuracies of various methods of radome analysis as functions of antenna size and placement, radome size and shape, and wavelength. The analytical methods used and the experimental program to establish true data are described concisely.			

DD FORM 1 JAN 73 1473

UNCLASSIFIED 40-21

SECURITY CLASSIFICATION OF THIS PAGE (When Data Entered)

1

(4)

DTIC  
REF

A  
1  
2  
3  
4  
5  
6  
7  
8  
9  
10  
11  
12  
13  
14  
15  
16  
17  
18  
19  
20  
21  
22  
23  
24  
25  
26  
27  
28  
29  
30  
31  
32  
33  
34  
35  
36  
37  
38  
39  
40  
41  
42  
43  
44  
45  
46  
47  
48  
49  
50  
51  
52  
53  
54  
55  
56  
57  
58  
59  
60  
61  
62  
63  
64  
65  
66  
67  
68  
69  
70  
71  
72  
73  
74  
75  
76  
77  
78  
79  
80  
81  
82  
83  
84  
85  
86  
87  
88  
89  
90  
91  
92  
93  
94  
95  
96  
97  
98  
99  
100

PARAMETRIC INVESTIGATION  
OF  
RADOME ANALYSIS METHODS

by

G. K. Huddleston, H. L. Bassett, and J. M. Newton

for

Air Force Office of Scientific Research  
Bolling Air Force Base, D.C. 20332

Under

Grant AFOSR-77-3469  
October 1, 1978 - September 30, 1979

School of Electrical Engineering  
and  
Engineering Experiment Station

Georgia Institute of Technology  
Atlanta, Georgia 30332

February 1980

Accession For	
NTIS E&I	<input checked="checked" type="checkbox"/>
DDC TAB	<input type="checkbox"/>
Unannounced	<input type="checkbox"/>
Justification	
By	
Department/	
Project/Activity Codes	
Dist	And/or special
A	

## TABLE OF CONTENTS

	<u>PAGE</u>
I. Introduction and Summary. . . . .	1
II. Progress to Date. . . . .	2
III. Presentations and Publications. . . . .	9
IV. Personnel and Interactions. . . . .	10
V. References. . . . .	12
APPENDIX A . . . . .	13
APPENDIX B . . . . .	23
APPENDIX C . . . . .	33

## LIST OF TABLES

<u>TABLE</u>		<u>PAGE</u>
1	Comparisons of Results Obtained for Radome Surface Integration Testing . . . . .	5
2	Ratios of $D_{is}/D_{ap}$ for Selected Antennas and Radomes. . . . .	6

## LIST OF ILLUSTRATIONS

<u>FIGURE</u>		
1	H-Plane Patterns for Azimuth Difference Channel of Medium Size Antenna with Radome (solid) and Without Radome (dashed). . . . .	8

## PARAMETRIC INVESTIGATION OF RADOME ANALYSIS METHODS

### I. Introduction and Summary

The overall objective of this research is to develop a general theory of radome analysis and to determine the accuracies of various radome analysis methods under controlled conditions of antenna size and placement, wavelength, and radome size and shape. Experimental measurements on selected antenna/radome combinations at 35 GHz will be used as true data in the assessment of accuracy.

During the first year a general theory of analysis was developed based on the Lorentz reciprocity theorem and on the Huygens-Fresnel principle. Computed-aided methods of analysis based on these principles were formulated and programmed. Three monopulse antennas were designed and fabricated for use in carrying out the measurements at 35 GHz. Three radomes were also designed and fabricated for use in the experimental program. A mechanical fixture was fabricated which allows accurate positioning of the antenna with respect to the radome and with respect to the reference system used for pattern measurements. A detailed discussion of the progress in the first year was presented in Reference 1.

During the second year, the initiation efforts of the first year's work have begun to come to fruition through concentrated experimental and analytical efforts to gather true and calculated data which will serve as the basis for realizing the overall research objective. Extensive pattern measurements have been made for nine of the fifteen antenna/radome combinations available. These experimental efforts have



been paralleled by computed-aided analyses of the same combinations for comparison purposes. In the process, a technique for synthesizing the aperture fields of the four-horn monopulse antennas from measured principal plane patterns has been developed. The progress during the second year is described in Section II below.

In the third year, measurements will be carried out on lens radomes and on conventional radomes to which metal tips have been added, and comparisons to theoretical predictions will be made. Antenna/radome configurations which lend themselves to exact analysis using boundary-valued approaches and modal expansions will be investigated.

Four publications and three presentations concerning this research have resulted. They are described in Section III along with papers planned for submission to technical journals.

The professional personnel associated with the research effort are listed in Section IV along with the interactions with DOD agencies and/or their contractors.

Appendix A contains copies of the papers presented at symposia. Appendix B contains Chapter 1 of a planned scientific report to be submitted for review in March.

## II. Progress to Date

Efforts during the second year have been made in both analytical and experimental areas. In the analytical area, the radome analysis computer programs have been finalized, and a method of monopulse antenna synthesis has been implemented to greatly facilitate the comparisons of computed and measured effects of the radomes on the antenna radiation patterns. In the experimental area, radiation pattern and boresight error measurements have been completed on the various combinations of antennas and radomes.

The radome analysis based on the Huygens-Fresnel principle [2] and Lorentz reciprocity [3] has been fully implemented in software and successfully tested for accuracy. The inner radome surface is used as the surface of integration. The normal voltage transmission coefficients are used to transform the incident plane wave from the outside surface to the inside surface  $S'$  where the surface integration is performed to obtain the voltage received by the antenna according to

$$V'_R(\hat{k}) = \int_{S'} (\underline{E}_T \times \underline{H}_R - \underline{E}_R \times \underline{H}_T) \cdot \hat{n} da \quad (1)$$

where the prime indicates integration over the radome surface.

Testing of the surface integration algorithms has been done by using an infinitely thin, "air" radome so that the surface integration is carried out over a tangent ogive surface in free space. The antenna is located at the base of the radome and consists of a square aperture excited with a  $TE_{10}$  waveguide mode so that the aperture fields,  $\underline{E}_{ap}$ ,  $\underline{H}_{ap}$ , are approximately Maxwellian. A plane wave is then assumed incident on the antenna/radome combination from the direction  $\hat{k}$ . The received voltage is computed according to Equation (1) and according to

$$V_R(\hat{k}) = \int_{S_{ap}} (\underline{E}_{ap} \times \underline{H}_R - \underline{E}_R \times \underline{H}_{ap}) \cdot \hat{n} da \quad (2)$$

where  $S_{ap}$  represents the aperture surface. By the Lorentz reciprocity theorem,

$$V_R(\hat{k}) - V'_R(\hat{k}) = \oint_{S' + S_{ap}} (\underline{E}_T \times \underline{H}_R - \underline{E}_R \times \underline{H}_T) \cdot \hat{n} da = 0 \quad (3)$$

Table 1 shows some results of this testing. A hemisphere ( $F=.5$ ) and a tangent ogive surface with fineness ratio  $F=1.0$  were used. The angles  $\phi$  and  $\theta$  specify the direction of arrival of the vertically polarized plane wave on the antenna ( $\hat{z}$  normal to the y-polarized aperture). Agreement is excellent.

The fields  $\underline{E}_T$ ,  $\underline{H}_T$  used in Equation (1) were computed from the specified aperture fields using the Huygens-Fresnel principle. Both magnetic ( $\underline{E}_{ap} \times \hat{n}$ ) and electric ( $\hat{n} \times \underline{H}_{ap}$ ) currents are used. Initially, it was intended that the plane wave spectrum (PWS) formulation [4] be used to compute these fields; however, its implementation has not yet been successful thus far. It has been established in a mathematically rigorous manner that the two formulations are entirely equivalent and should indeed yield the same results. Work is continuing in this area because the PWS approach may offer a speed advantage in the computations.

Another important analytical endeavor, and one that has required considerable time, is the development and implementation of an aperture synthesis method using measured principal plane patterns as described in Appendix A. Using this technique, antenna aperture fields are generated from the measured far-field patterns such that when they are used in the radome analysis, the measured patterns will be predicted exactly in the absence of the radome. Then, when the patterns are computed with the radome in place and compared to their experimental counterparts, valid comparisons can be made between the accuracies of three radome analysis methods under investigation. The synthesis technique has much broader application and is currently being investigated for two-dimensional synthesis using measured near-field data [5].

Numerous pattern and boresight error measurements have been made on the eight antenna/radome combinations shown in Table 2. (The large

Table 1. Comparisons of Results Obtained for  
Radome Surface Integration Testing

Finess Ratio	$\phi$ (deg.)	$\theta$ (deg.)	$V_R'$		$V_R$		No. of Points/ Computation Time(sec.)
			Amp.(dB)	Phase( $^{\circ}$ )	Amp(dB)	Phase( $^{\circ}$ )	
.5	0	0	0.00	180.	0.00	180.	162/11.69
.5	0	15	-4.94	179.	-5.11	-180.	162/12.01
.5	90	15	-8.22	-180.	-8.32	-180.	162/12.33
1.0	0	0	0.00	180.	0.00	180.	229/17.53
1.0	0	15	-4.95	180.	-5.11	-180.	229/17.91
1.0	90	15	-8.25	-179.	-8.32	-180.	229/17.48

Table 2. Ratios of  $D_{is}/D_{ap}$  for Selected Antennas and Radomes

<u>Radome</u>	<u>Antenna</u>		
	<u>Small</u>	<u>Medium</u>	<u>Large</u>
Small (F=1)	2.33*	--	--
Medium (F=1)	3.98*	2.33*	1.27
Medium (F=1.5)	--	2.33*	--
Medium (F=2.0)	--	2.33*	--
Large (F=1)	7.28*	4.27*	2.33*

\* Measurements completed.

antenna would not fit inside the medium radome.) For each antenna/radome combination, eight patterns were measured for each of the three channels of the four-horn monopulse antenna: four pattern cuts ( $\phi=0$ ,  $45^\circ$ ,  $90^\circ$ , and  $135^\circ$ ) and two polarizations. In addition, boresight error measurements were made for each combination as allowed by the special positioner used.

All the patterns were made on a pattern range in the usual manner; however, considerable effort was spent in translating the data from pattern recording paper to computer files for easy access during the comparison phase. This translation was done using an xy digitizer and HP2100 minicomputer system at the Engineering Experiment Station. After the data were digitized and stored in files on the HP2100, they were transferred to the central campus computer (Cyber 70/74) where the analyses are being done.

Plotting software has been developed on the Cyber for overlaying various patterns on the same axes for comparison purposes. An example is shown in Figure 1 for the azimuth difference channel of the medium antenna inside the medium radome: the solid line is the pattern with the radome; the dashed is the pattern of the antenna without the radome (for reference).

At the present time, the aperture fields for the three antennas are being synthesized using measured pattern data such as that shown in Figure 1. The analyses will be run next and comparisons made between measured and computed results. From these comparisons, the accuracies and ranges of validity of the fast receiving, fast transmitting, and surface integration methods of analysis will be determined.

During the third year (which is already in progress), three topics are of interest: radomes with metal tips, lens radomes, and antenna/

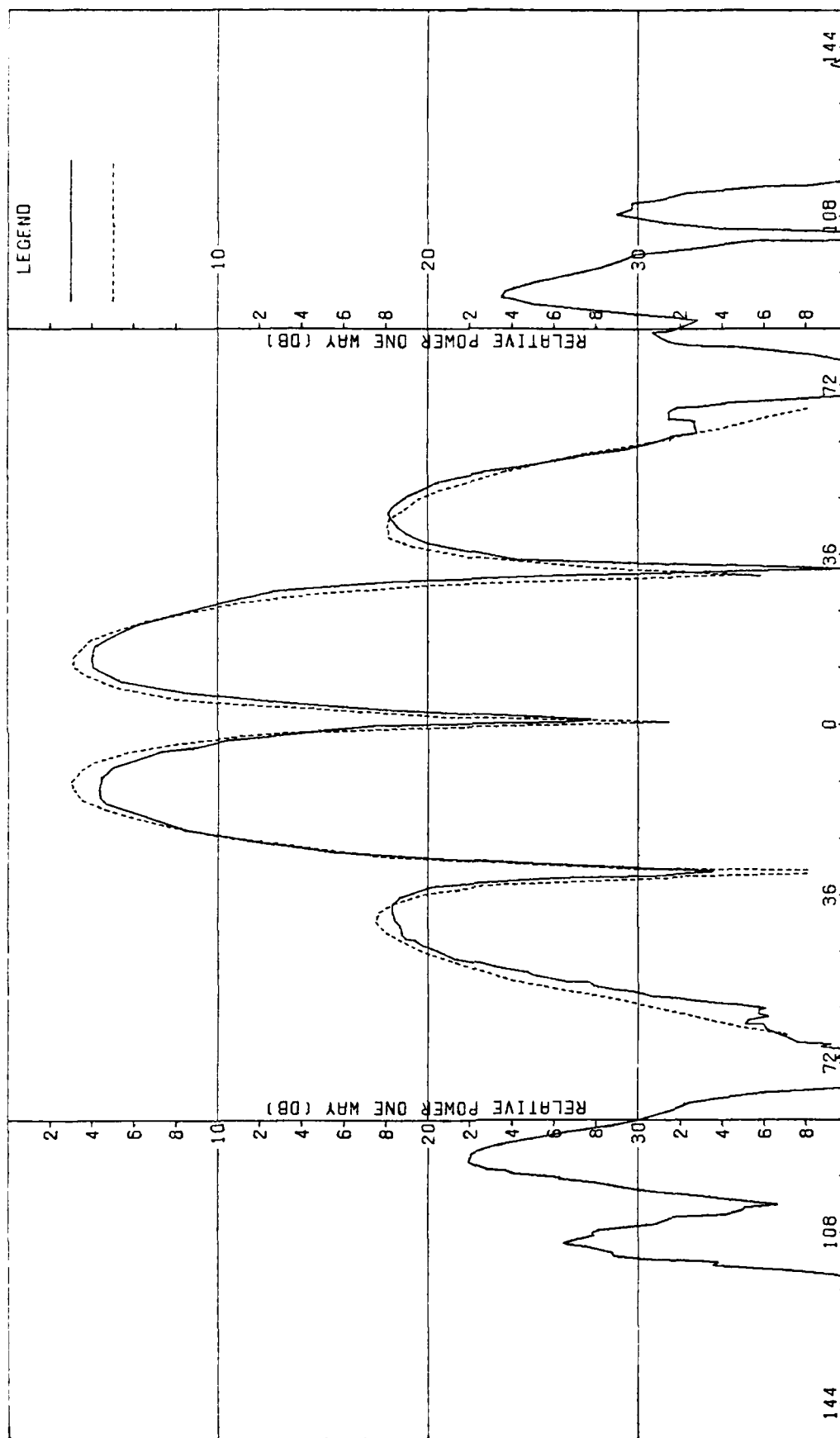


Figure 1. H-Plane Patterns for Azimuth Difference Channel of Medium Size Antenna with Radome (solid) and Without Radome (dashed).

radome configurations which lend themselves to exact analysis. The three medium sized radomes having fineness ratios of 1, 1.5, and 2 will be fitted with metal tips, and measurements and analytical comparisons will be made. The analysis software will be modified to accommodate lens radomes, and measurements will be carried out on two lenses. Finally, the boundary-value problem of a perfectly conducting sphere inside a concentric spherical dielectric shell will be solved to serve as a model for generating exact analytical data for general use in accessing the accuracy of any computer-aided radome analysis method.

### III. Presentations and Publications

G. K. Huddleston, H. L. Bassett, and J. M. Newton, "Parametric Investigation of Radome Analysis Methods," Presented at and published in Proceedings of 1978 IEEE AP-S Symposium and Proceedings of Fourteenth Symposium on Electromagnetic Windows.

G. K. Huddleston, "Radome Analysis," invited presentation to Atlanta Chapter of IEEE, AP-S/MTT Group.

G. K. Huddleston, H. L. Bassett, and J. M. Newton, "Parametric Investigation of Radome Analysis Methods," Annual Technical Report, AFOSR, November 1978.

G. K. Huddleston, "Equivalence of Receiving and Transmitting Formulations of Radome Analysis," Paper to be submitted to IEEE AP-S Transactions (see Appendix A).

G. K. Huddleston, "A General Theory of Radome Analysis," Paper in preparation for submission to IEEE AP-S Transactions.

G. K. Huddleston and I. Rusodimos, "Computed-Aided Radome Analysis Using Geometrical Optics and Lorentz Reciprocity," AFOSR Scientific Report, planned for submission in March 1980 (see Appendix B).

G. K. Huddleston and I. Rusodimos, "Computed-Aided Radome Analysis Using Huygens-Fresnel Principle and Lorentz Reciprocity," AFOSR Scientific Report, planned for submission in April 1980.

G. K. Huddleston, "Aperture Synthesis From Principal Plane Patterns of Monopulse Antenna for Radome Analysis," submitted to 1980 IEEE/AP-S Symposium, June 1980 (see Appendix A).



G. K. Huddleston, H. L. Bassett, and J. M. Newton, "Parametric Investigation of Radome Analysis Methods: Experimental Results," AFOSR Scientific Report, planned for submission April 1980.

G. K. Huddleston, H. L. Bassett, and J. M. Newton, "Parametric Investigation of Radome Analysis Methods: Comparisons of Analytical and Experimental Results," AFOSR Scientific Report, planned for submission June 1980; also planned for submission as paper to IEEE Transactions on Antennas and Propagation.

#### IV. Personnel and Interactions

The following professional personnel are actively engaged in this research program:

G. K. Huddleston	Assistant Professor	School of Electrical Engineering
H. L. Bassett	Senior Research Engineer	Engineering Experiment Station
J. M. Newton	Research Engineer	Engineering Experiment Station

Dr. Huddleston and Mr. Bassett serve as co-principal investigators.

Dr. Huddleston directs the analytical efforts while Mr. Bassett directs the experimental work. Mr. Jason Rusodimos, a graduate student in the School of Electrical Engineering worked with Dr. Huddleston on the computer implementation of various analysis methods. Mr. William Adams, a co-operative student, has worked closely with Mr. Newton in the measurements program.

Interactions have taken place with DOD agencies and/or their contractors. Software has been delivered to Naval Surface Weapons Center, Dahlgren, Virginia, (Richard M. Swink) for use in assessing the performance of a new shipboard radome design. Radome analysis computer programs have been documented and installed on the IBM 3033 system at Applied Physics Laboratory, Laurel, Maryland, (R. C. Mallalieu) for use in a significant radome technology program for the Department of the Navy. The

fast receiving formulation software has been delivered to Flight Systems, Inc., Newport Beach, California, (Bernard Crowe) for general radome analysis work in the ECM area. This software has also been installed on the SEL system at Georgia Tech Engineering Experiment Station (H. L. Bassett) and is being used in a polarimetric study for the U. S. Army Missile Command. Discussions are currently underway with China Lake Test Center (Joseph Mosko) and Texas Instruments, Inc. (Dave Burks) concerning this radome work.

Three other developments are noteworthy. First, the School of Electrical Engineering has recently become a member of the Joint Services Electronics Program, and Dr. Huddleston will be carrying out an investigation to determine, by measurement, the electromagnetic fields on the surface of a radome. Second, a specialized research equipment grant has been received from the National Science Foundation to establish an Automated Radiation Laboratory in the School of Electrical Engineering for use in carrying out antenna and radome research. Finally, an advanced graduate course on radome analysis was taught last Fall by Dr. Huddleston (see Appendix C).

It is important to note that the AFOSR grant support has been catalytic and instrumental in the success of these auxiliary radome-related activities, and that support is hereby gratefully acknowledged.

V. References

1. G. K. Huddleston, H. L. Bassett, and J. M. Newton, "Parametric Investigation of Radome Analysis Methods," Annual Technical Report, AFOSR-77-3469, November 1978.
2. Samuel Silver, ed., Microwave Antenna Theory and Design, Section 3-8, McGraw-Hill, New York, 1949.
3. R. E. Collin and F. J. Zucker, "Antenna Theory, Part 1," Sections 4.2 and 4.5, McGraw-Hill, New York, 1969.
4. P. C. Clemmow, The Plane Wave Spectrum Representation of Electromagnetic Fields, Pergamon Press, Oxford, 1966.
5. E. B. Joy and T. S. Craven, "Accuracy of Radiation Patterns Determined From Spatially-Limited Near-Field Measurements," National Science Foundation grant, on-going.

Appendix A

Publications

APERTURE SYNTHESIS FROM PRINCIPAL PLANE PATTERNS  
OF MONOPULSE ANTENNA FOR RADOME ANALYSIS

G. K. Huddleston  
School of Electrical Engineering  
Georgia Institute of Technology  
Atlanta, Georgia 30332

Valid comparisons of the accuracies of radome analysis [1] using measured radiation patterns as true data require that each analysis method be capable of predicting exactly the antenna patterns measured in the absence of the radome. When the measured amplitude and phase of the antenna fields are known over the complete sphere, an aperture synthesis method such as that described by Ludwig [2] can be used. But when the measured data is limited to amplitude-only, principal plane patterns, a different approach and one which exploits all available information about the antenna to be synthesized, must be used.

Such a method of aperture synthesis for a four-horn monopulse antenna using principal plane amplitude patterns of the sum and two difference channels is described. The radius ( $a=.74\lambda$ ) and element half-spacing ( $d_x=d_y=.95\lambda$ ) of each vertically (y) polarized conical horn element ( $10^\circ$  flare angle) are also used in the procedure. The accuracy of the method is illustrated below for a theoretical array. Synthesis results obtained using measured data, and analysis results with the radome in place, will be presented at the symposium.

Theory

The synthesis procedure is carried out independently in the two principal planes to determine the plane wave spectra  $A_{xe}, A_{ye}$  and aperture fields  $E_{xe}, E_{ye}$  of each identical element in the four-horn array. Pattern separability and ideal element excitation are additional necessary assumptions. Starting with the general expression for the radiation field of the array in wavenumber coordinates,

$$\begin{aligned} \underline{E}_{ff}(k_x, k_y) = \underline{E}_{eff}(k_x, k_y) [ & a_1 e^{j\beta_0(d_x k_x + d_y k_y)} + a_2 e^{j\beta_0(-d_x k_x + d_y k_y)} \\ & + a_3 e^{-j\beta_0(d_x k_x + d_y k_y)} + a_4 e^{-j\beta_0(-d_x k_x + d_y k_y)} ], \end{aligned} \quad (1)$$

it can be shown that the H-plane plane wave spectra of the element may be found from

$$A_{xe}(k_x, 0) = \frac{V_{\theta\Sigma}(k_x, 0) + V_{\theta\Delta\Delta Z}(k_x, 0)}{(1+k_z)(4 \cos\beta_o \frac{d}{x} k_x + 2 \sin\beta_o \frac{d}{x} k_x)} \quad (2)$$

$$A_{ye}(k_x, 0) = \frac{V_{\theta\Sigma}(k_x, 0) + V_{\phi\Delta\Delta Z}(k_x, 0)}{(1+k_z)(4 \cos\beta_o \frac{d}{x} k_x + 2 \sin\beta_o \frac{d}{x} k_x)} \quad (3)$$

where the numerators are the measured amplitude data and where  $k_x = \sin\theta$  in the H-plane. Similar expressions hold for the E-plane.

The above expressions for  $A_{xe}, A_{ye}$  are valid only over the range  $k_x = \pm 1$ ; i.e.,  $\theta = \pm 90^\circ$ . In order to obtain (via Fourier transform) the corresponding element aperture fields, evanescent energy must be added to the plane wave spectra according to well-defined criteria [3]. The criteria adopted here is that the element aperture fields are limited in spatial extent to the circular region occupied by the horn aperture; i.e.,  $A_{xe}, A_{ye}$  are band-limited.

The first estimate to the field  $E_{xnf}(x, 0)$  is obtained by Fourier transforming  $A_{xe}(k_x, 0)$ . Energy outside  $|x| \leq a$  is truncated, and the resulting field is inverse transformed to yield a spectrum  $A'_{xe}(k_x, 0)$ . The energy outside  $|k_x| \leq 1$  is taken as the first estimate to the evanescent energy of  $A_{xe}$ . This evanescent energy is added to  $A_{xe}$ , and the process is repeated until a very high percentage of energy in  $E_{xnf}$  is concentrated in the region  $|x| \leq a$ . The procedure is repeated for the other field component. A complete element aperture field can be obtained to within a multiplicative constant as  $E_{xe}(k_x, k_y) = E_{xe}(k_x, 0) E_{ye}(0, k_y)$ .

### Results

Figure 1 shows a comparison of the true and synthesized difference elevation patterns for a four-horn array. The true data were generated using a  $TE_{11}$  circular waveguide mode in each element. The mode was rotated  $5^\circ$  from the vertical to produce the low amplitude cross (x) component. Concentration factors of  $(1.-10^{-5})$  and  $(1.-10^{-2})$  were obtained for the primary (y) and cross (x) components, respectively, to produce the excellent synthesis results shown.

### Acknowledgement

This research is sponsored by the Air Force Office of Scientific Research under Grant AFOSR-77-3469. The United States Government is authorized to reproduce and distribute reprints for governmental purposed notwithstanding any copyright notation hereon.

The help of Professor R. W. Schafer in defining the method of adding evanescent energy to the plane wave spectrum is gratefully acknowledged.

#### References

1. G. K. Huddleston, H. L. Bassett, and J. M. Newton, "Parametric Investigation of Radome Analysis Methods", 1978 IEEE AP-S Symposium Digest, pp. 199-201, May 1978.
2. A. C. Ludwig, "Radiation Pattern Synthesis for Circular Aperture Horn Antennas", IEEE Trans., AP-14, No. 4, pp. 434-440, July 1966.
3. A. Papoulis, "A New Algorithm in Spectral Analysis and Band-Limited Extrapolation", IEEE Trans., CAS-22, No. 9, pp. 1299-1306, September 1975.

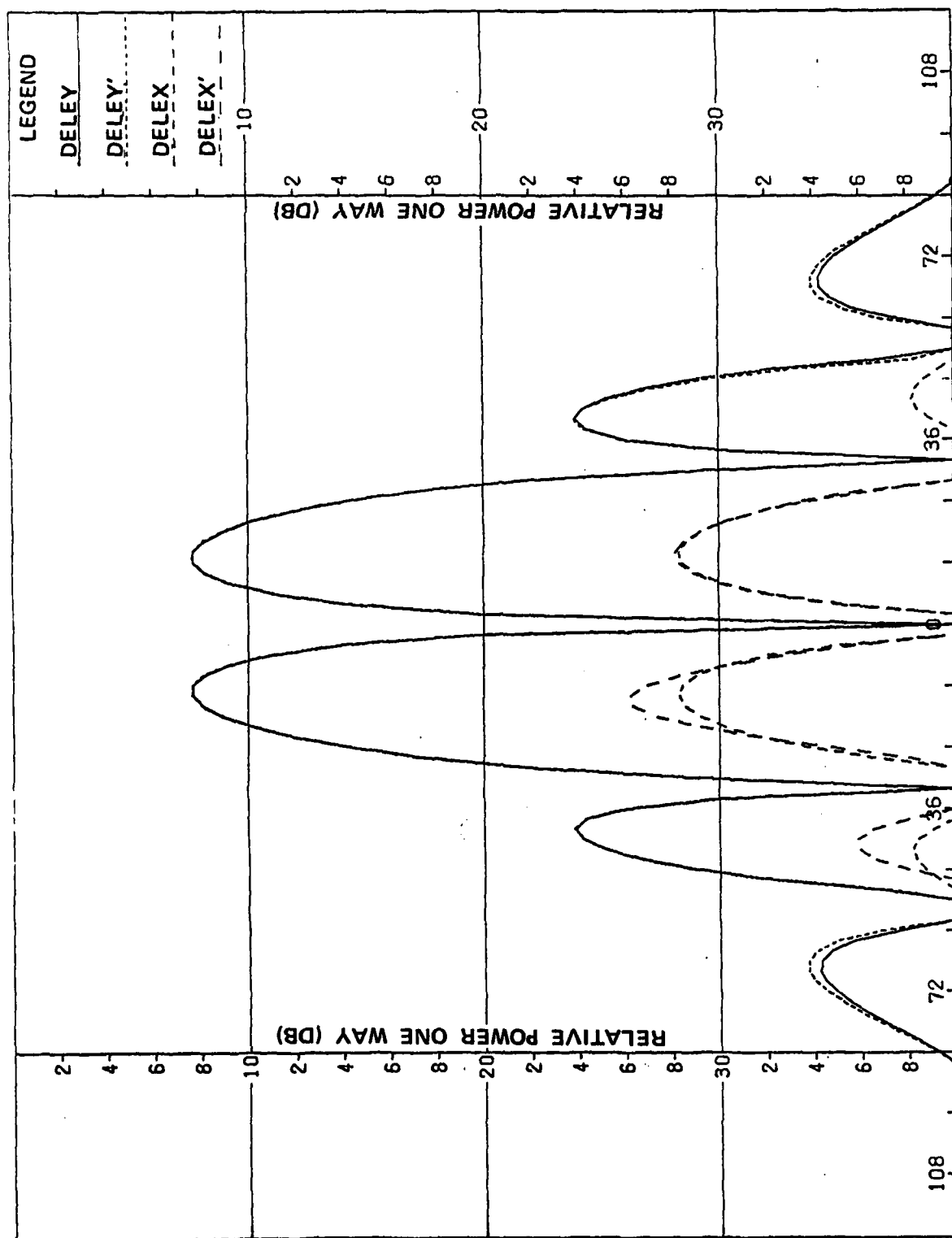


FIGURE 1. COMPARISON OF TRUE AND SYNTHESIZED (') E-PLANE DIFFERENCE PATTERNS OF FOUR-HORN MONOPULSE ANTENNA.



# EQUIVALENCE OF RECEIVING AND TRANSMITTING FORMULATIONS IN RADOME ANALYSIS

G. K. Huddleston  
Georgia Institute of Technology  
School of Electrical Engineering  
Atlanta, Georgia 30332

It is well known that the receiving and transmitting patterns of an antenna in free space are identical. In what follows, it is theoretically demonstrated that the receiving and transmitting patterns for an antenna enclosed by a dielectric radome are also identical, and that the receiving and transmitting formulations of radome analysis [1] lead to identical results.

The Huygens-Fresnel principal [2] and the Lorentz reciprocity theorem [3] are used to establish the equivalence. The theory is then applied to show that the effect of the scattered fields on receiving response is identically zero. A method is suggested whereby discrepancies caused by an unrealizable edge condition for an aperture illumination function can be resolved for the receiving case by utilizing results already obtained for the transmitting case [4].

## Theory

Consider a linear antenna operating in the sinusoidal steady state ( $e^{j\omega t}$  time variations suppressed) and enclosed by a dielectric radome. Let a closed outer surface  $S$  coincide with the outer surface of the radome so that when the antenna is energized, the electric field at any point  $(x', y', z')$  outside the radome is given by [2].

$$\underline{E}(x', y', z') = \frac{1}{4\pi} \oint_S [-j\omega\mu\psi(\hat{n} \times \underline{H}_T) + (\hat{n} \times \underline{E}_T) \times \underline{\nabla}\psi + (\hat{n} \cdot \underline{E}_T)\underline{\nabla}\psi] ds \quad (1)$$

where  $\underline{E}_T, \underline{H}_T$  are the fields produced on  $S$  by the antenna,  $\hat{n}$  is a unit vector normal to  $S$  and pointing into the unbounded region, and  $\psi$  is the free-space Green's function

$$\psi = \frac{e^{-jkr}}{r} \quad (2)$$

and where  $r$  is the distance from the (equivalent) source point  $(x, y, z)$

on  $S$  to the point of observation  $(x', y', z')$  as illustrated in Figure 1. For the directions assigned to the unit vectors  $\hat{r}$  and  $\hat{R}$  in Figure 1, the expression for gradient  $\psi$  is [2]

$$\underline{\nabla}\psi = (jk + \frac{1}{r}) \frac{e^{-jkr}}{r} \hat{r} \quad (3)$$

where  $k = 2\pi/\lambda$  and where  $\lambda$  is the wavelength. The constitutive parameters of the homogeneous unbounded medium are  $\epsilon$  and  $\mu$ .

After Collin [5], let an infinitesimal current element of strength  $I_b$ , length  $\Delta\ell$ , and orientation  $\hat{n}_b$  be located at  $(x', y', z')$ . Let the fields produced on  $S$  by the current element be given by  $\underline{E}_R, \underline{H}_R$ . An application of the reciprocity theorem to the unbounded region yields

$$\oint_S (\underline{E}_T \times \underline{H}_R - \underline{E}_R \times \underline{H}_T) \cdot \hat{n} dS = - \underline{E} \cdot \hat{n}_b I_b \Delta\ell \quad (4)$$

A second application of the reciprocity theorem to the source-free volume  $V'$  inside the radome enclosed by  $S$  and by a surface  $S'$  surrounding the antenna yields the result that the complex voltage response  $V_R$  of the antenna to the fields  $\underline{E}_R, \underline{H}_R$ , incident on  $S$  is proportional to the integral in Equation (4); hence,

$$V_R = I_b \Delta\ell \underline{E} \cdot \hat{n}_b = C \int_S (\underline{E}_T \times \underline{H}_R - \underline{E}_R \times \underline{H}_T) \cdot \hat{n} dS \quad (5)$$

where  $\underline{E}$  is given by Equation (1) in the absence of the current element and where  $C$  is a complex constant.

When the point of observation is a great distance  $R$  from the origin  $O$  of source coordinates, the fields  $\underline{E}_R, \underline{H}_R$  produced on  $S$  by the current element are those of a plane wave propagating in the  $-\hat{R} = \hat{k}_a$  direction, and  $\underline{H}_R$  is given by

$$\underline{H}_R = \frac{\underline{E}_R \times \hat{R}}{\eta} = \frac{\hat{k}_a \times \underline{E}_R}{\eta} \quad (6)$$

where  $\eta$  is the intrinsic impedance of the unbounded medium. The constant  $C$  in Equation (5) can be chosen so that  $\underline{E}_R$  is given by

$$\underline{E}_R = j\omega\mu \frac{e^{-jkR}}{R} \hat{n}_b e^{j\hat{k}\hat{a} \cdot \underline{r}'} \quad (7)$$

where  $\underline{r}'$  is the position vector from the origin 0 to the source coordinates  $(x, y, z)$  as shown in Figure 1. The magnetic field follows from Equations (6) and (7) as

$$\underline{H}_R = jk \frac{e^{-jkR}}{R} e^{j\hat{k}\hat{a} \cdot \underline{r}'} (\hat{n}_b \times \hat{R}) \quad (8)$$

where the relation  $k = \omega\mu/\eta$  has been used.

The next step in the development consists of evaluating Equation (5) using the expression for  $\underline{E}$  from Equation (1), under the condition of large  $R$ ; i.e., far-field approximation. When this is done, the response of the antenna to the incident plane wave is given by

$$\begin{aligned} V_R = \frac{I_b \Delta \ell}{4\pi} \int_S [-j\omega\mu \frac{e^{-jkR}}{R} e^{j\hat{k}\hat{a} \cdot \underline{r}'} \hat{n}_b \cdot (\hat{n} \times \underline{H}_T + \hat{n}_b \cdot (\hat{n} \times \underline{E}_T) \\ \times \hat{R} \frac{jke^{-jkR}}{R} e^{j\hat{k}\hat{a} \cdot \underline{r}'} + \hat{n}_b \cdot \nabla \psi_{ff} (\hat{n} \cdot \underline{E}_T)] dS \end{aligned} \quad (9)$$

Where the following asymptotic relations have been used:

$$\underline{r} \sim R - R \cdot \underline{r}' \quad (10)$$

$$\frac{e^{-jkr}}{r} \sim \frac{e^{-jkR}}{R} e^{j\hat{k}\hat{a} \cdot \underline{r}'} \quad (11)$$

$$\nabla \psi \sim \nabla \psi_{ff} = \hat{R}jk \frac{e^{-jkR}}{R} e^{j\hat{k}\hat{a} \cdot \underline{r}'} \quad (12)$$

Using the vector identity  $\underline{a} \cdot \underline{b} \times \underline{c} = \underline{b} \cdot \underline{c} \times \underline{a}$ , the first term  $T_1$  in the integrand of Equation (9) can be written as

$$T_1 = -j\omega\mu \frac{e^{-jkR}}{R} \hat{n} \cdot \underline{H}_T \times \hat{n}_b e^{j\hat{k}\hat{a} \cdot \underline{r}'} \quad (13)$$

Comparison to Equation (7) reveals that

$$T_1 = \underline{E}_R \times \underline{H}_T \cdot \hat{n} \quad (14)$$

i.e.,  $T_1$  is identical to the second term in the integrand of Equation (5).

Repeated application of the same vector identity to the second term  $T_2$  in the integrand of Equation (9) yields

$$T_2 = \hat{n} \cdot [\underline{E}_T \times (\nabla \psi_{ff} \times \hat{n}_b)] \quad (15)$$

or

$$T_2 = \hat{n} \cdot [\underline{E}_T \times (jk \frac{e^{-jkr}}{R} e^{jk \hat{k}_a \cdot \underline{r}'} \hat{R} \times \hat{n}_b)] \quad (16)$$

Comparison of the expression in parenthesis in Equation (16) with Equation (8) shows that  $T_2$  is equal to the negative of the first term in Equation (5). Collecting results yields the desired final result as

$$\begin{aligned} V_R &= C \int_S (\underline{E}_T \times \underline{H}_R - \underline{E}_R \times \underline{H}_T) \cdot \hat{n} dS = \hat{n}_b \cdot \underline{E} \\ &= \hat{n}_b \int_S [-j\omega\mu\psi(\hat{n} \times \underline{H}_T) + (\hat{n} \times \underline{E}_T) \times \nabla \psi_{ff} + (\hat{n} \cdot \underline{E}) \nabla \psi] dS \end{aligned} \quad (17)$$

for the case of large  $R$  (far-field approximation). It is noted that the third term in Equation (9) is identically zero since  $\hat{n}_b$  is perpendicular to  $\nabla \psi_{ff}$ .

The result in Equation (17) establishes that the receiving and transmitting patterns of the antenna/radome combination are identical. Furthermore, it establishes the equivalence of the receiving and transmitting formulations of radome analysis under far-field conditions. The analysis also shows the conditions of equivalence; viz., that the fields on the outer surface of the radome must be known. In this respect, the receiving formulation may offer some advantages over the transmitting formulation since it does not depend on the existence of a homogeneous unbounded medium outside the surface  $S$ .

#### Application

A concise application of the foregoing analysis is to show that the response of the antenna to a plane wave depends on only the

incident field  $\underline{E}_R^i, \underline{H}_R^i$  and not on the scattered fields  $\underline{E}_R^S, \underline{H}_R^S$ . Examination of Equation (9) shows directly that only the incident plane wave is involved. This is, of course, in keeping with the reciprocity theorem in that

$$\oint_S (\underline{E}_T \times \underline{H}_R^S - \underline{E}_R^S \times \underline{H}_T) \cdot \hat{n} dS \equiv 0 \quad (18)$$

when the source free volume V is considered.

A second application of the analysis concerns the problem of resolving differences in responses for aperture distributions having bounded support by using line charge distributions. For the transmitting case, the method of Stratton and Chu [4] can be readily utilized. Moreover, the same method can be applied in the receiving case by utilizing the above analysis results as will be done in a later paper.

#### Acknowledgement

This research is sponsored by the Air Force Office of Scientific Research under Grant No. AFOSR-77-3469. The United States Government is authorized to reproduce and distribute reprints for governmental purposes notwithstanding any copyright notation hereon.

#### References

1. G. K. Huddleston and H. L. Bassett, "Parametric Investigation of Radome Analysis Methods," 1978 IEEE APS Symposium Digest, pp. 199-201, May 1978.
2. Samuel Silver (ed.), Microwave Antenna Theory and Design, New York, New York: McGraw-Hill Book Company, 1949, Section 3-8.
3. G. D. Monteath, Applications of the Electromagnetic Reciprocity Principle, New York. New York: Pergamon Press, 1973.
4. J. A. Stratton and L. J. Chu, "Diffraction Theory of Electromagnetic Waves," Physical Review, 56, pp. 99-107, July 1, 1939.
5. R. E. Collin and F. J. Zucker, Antenna Theory, Part 1, New York, New York: McGraw-Hill Book Company, 1969, Ch. 4.

Appendix B

Excerpts from Planned AFOSR Scientific Report

"Computer-Aided Radome Analysis Using Geometrical Optics  
and Lorentz Reciprocity"

# TABLE OF CONTENTS

	<u>PAGE</u>
LIST OF ILLUSTRATIONS. . . . .	iii
LIST OF TABLES . . . . .	vi
CHAPTER	
1. Introduction and Summary. . . . .	1
2. PROGRAM RTFRACP . . . . .	9
3. SUBROUTINE HACNF. . . . .	57
4. SUBROUTINE ORIENT . . . . .	71
5. SUBROUTINE POINT. . . . .	81
6. SUBROUTINE VECTOR . . . . .	85
7. SUBROUTINE INCPW. . . . .	89
8. SUBROUTINE RECM . . . . .	95
9. SUBROUTINE TRACE. . . . .	111
10. SUBROUTINE RXMIT. . . . .	117
11. SUBROUTINE WALL . . . . .	129
12. SUBROUTINE AXB. . . . .	135
13. SUBROUTINE CAXB . . . . .	137
14. SUBROUTINE RECBS. . . . .	139
15. SUBROUTINE RECPTN . . . . .	151
16. SUBROUTINE OGIVE. . . . .	157
17. SUBROUTINE OGIVEN . . . . .	169
18. SUBROUTINE XY . . . . .	173
19. SUBROUTINES BDISK, BDISKN, TDISK, TDISKN. . . . .	177
20. SUBROUTINE FAR. . . . .	183

CHAPTER	<u>PAGE</u>
21. SUBROUTINE AMPHS. . . . .	195
22. SUBROUTINE DBPV . . . . .	197
23. SUBROUTINE NORMH. . . . .	199
24. SUBROUTINE CNPLTH AND FUNCTION PSI. . . . .	205
25. SUBROUTINES PLT3DH AND PLTT . . . . .	213
26. SUBROUTINE FFTA . . . . .	221
27. SUBROUTINE MAGFFT . . . . .	235
28. SUBROUTINE JOYEFT . . . . .	239
APPENDICES	
A. Test Case 1 for RTFRACP . . . . .	249
B. Test Case 2 for RTFRACP . . . . .	253
C. Test Case 3 for RTFRACP . . . . .	287
D. Test Case 4 for RTFRACP . . . . .	291
E. Plane Wave Transmission Through Multilayered Radome Wall. . .	323



## Chapter 1

### INTRODUCTION AND SUMMARY

#### 1-1. Introduction

This report documents a ray tracing radome analysis computer program written in Fortran IV for use on the IBM 3033 computing system at Johns Hopkins University Applied Physics Laboratory. The program was developed at Georgia Institute of Technology over the past four years; however, considerable development work in computer aided radome analysis has taken place here prior to that time [1-7].

This analysis package is intended to support the on-going radome technology program at APL and is documented herein for that purpose; however, it is important to point out that this effort was done in conjunction with the on-going radome analysis work at Georgia Tech under grant AFOSR-77-3469[8]. It is anticipated that this report will be available to other government contractors through the National Technical Information Service as part of the technology transfer functions of the supporting agencies.

The report is organized by chapters according to the approximate order in which the subprograms are called, and each chapter describes one subprogram. Each chapter is essentially self-contained since it is meant to serve as the complete documentation on a single subroutine. References are provided at the end of each chapter. In some cases, figures are duplicated in different chapters for completeness. Each chapter is terminated with the listing of the subroutine.

Chapter 2 describes the main program and instructions for its use. Chapters 3 through 28 describe the thirty four subroutines required for execution, including those for producing Calcomp pattern plots and three-dimensional plots. Appendices A through D present computed results for four test cases for use in verifying correct operation on other systems. These results were obtained on the Cyber 70/74 computing system at Georgia Tech. The remaining part of this chapter describes background of the program development and summarizes the features of the computer analysis.

Two companion reports are also of interest [9, 10]. In the first, a method of analysis based on the Huygens-Fresnel principle (surface integration) is described which makes use of most of the computer software described in the present report. The second report compares the results obtained using these two computer-aided analyses with those obtained experimentally at 35 GHz for various combinations of sizes of monopulse antennas and tangent ogive radomes [8]. The latter report represents the culmination of this radome analysis research.

#### 1-2. Background

Development of the radome analysis computer program (RACP) was initiated in 1971 in an effort to include the effects of the radome on a ground mapping radar [1]. A three-dimension geometry and vector field formulation were used. A plane wave spectrum (PWS) representation of the radiation from the antenna greatly facilitated the computations since the Fast Fourier Transform (FFT) could be used. The program was used to compute power patterns on the ground for many different cases of antenna/missile orientations. From these data, the effects of the radome on pattern shape, power loss and VSWR were determined.

Monopulse tracking antennas were next introduced into the computer analysis to evaluate radome materials and shapes for seeker systems in the 8-18 GHz band [2]. Tangent ogive shapes of various fineness ratios were analyzed. Monolithic and multilayer wall structures were used. Algorithms were developed to compute boresight errors from the sampled data difference patterns in two orthogonal planes. A modification of this program was also used to conduct a trade-off and development study for the Multipurpose Missile (MPM), later known as ASALM [3].

The next step in the development of RACP came in 1977 with the introduction of a conical scan tracking antenna into the analysis [4]. This antenna necessitated a reformulation of the analysis from the transmitting formulation used earlier to a receiving formulation. The big advantage offered by the latter is that the antenna response can be calculated for only one direction of arrival of the target return (plane wave). In the former, the FFT automatically computes "responses" for many directions of arrival and, hence, is computationally slower. Subsequent versions of the program have used the same receiving formulation with monopulse and other types of antenna models.

The computed results obtained with the receiving and transmitting formulations are not always the same [5]. A computed-aided analysis which utilizes the Huygens-Fresnel principle [6, 7] is generally considered to be more accurate than the two methods already mentioned, but requires considerably more computation time that may not be warranted in all cases. A research program is now underway at Georgia Tech whose objective is to establish the accuracies and ranges of validity of these three methods of radome analysis [5].

### 1-3. Description of the Analysis

The current version of the ray tracing analysis computer program utilizes a receiving formulation based on the Lorentz reciprocity theorem [5]. A plane wave of selectable linear or circular polarization is assumed incident on the outside of the radome and is represented by a system of parallel rays. There is one ray for each sample data point in the antenna aperture inside the radome. Each ray is traced from the point where it impinges on the outside surface to the corresponding aperture point. The electric and magnetic fields  $\underline{E}_1$ ,  $\underline{H}_1$  associated with each ray are weighted by the flat panel transmission coefficients  $T_\perp$ ,  $T_\parallel$  as determined by the unit normal  $\hat{n}$ , the direction of propagation  $\hat{k}$ , and the dielectric properties of the radome wall. The weighted incident fields  $\underline{E}'_1$ ,  $\underline{H}'_1$  at each aperture point are then used in the following integral to obtain the complex voltage response  $V_r$  of the antenna as

$$V_r = C \iint_S (\underline{E}_T \times \underline{H}'_1 - \underline{E}'_1 \times \underline{H}_T) \cdot \hat{z} \, dx dy \quad (1)$$

where  $\underline{E}_T$ ,  $\underline{H}_T$  are the aperture fields when the antenna is transmitting,  $C$  is a complex constant, and  $\hat{z}$  is the unit vector normal to the  $xy$  (aperture) plane. For digital computer implementation, the integral in Equation (1) reduces to a double summation, and the equal-area elements  $dx dy$  become  $\Delta x \Delta y$  and can be absorbed into the constant  $C$ .

In its present form, the program accommodates only one radome shape; viz., the tangent ogive. The length, diameter and fineness ratio are, of course, all variable in the input data. Monolithic and multi-layer wall configurations can be analyzed; however, only uniform wall configurations whose properties do not vary from point to point on the

wall can be handled. Provisions are made to allow for a metal tip on the radome whose effect is aperture blockage.

The geometry subroutines provide for three separate coordinate systems and the point and vector transformations among them. A reference coordinate system is provided to orient the antenna/radome combination with respect to other bodies. The coordinate systems for the antenna and the radome comprise the other two systems. Boresight error and pattern computations are carried out and expressed in the antenna coordinate system.

The primary outputs of the program are boresight error (mrad.), boresight error slope (deg./deg.), gain loss, and when selected, principal plane patterns. Outputs include both printing and plotting (Calcomp). Plotting options allow for selection of aperture fields with and without the radome. A feature is also provided to either obtain or suppress intermediate calculated results for debugging purposes.

Boresight error calculations for monopulse antennas are carried out by setting the first target return at a known direction within a few degrees of true boresight. The responses in the two difference channels and the sum channel are then computed and stored. Another set of responses for a return  $180^\circ$  away from the first is computed next. The two sets of data are then used to construct a linear tracking model in the two orthogonal planes, and the process is repeated until a boresight null is indicated. The true direction of arrival of the plane wave at this point represents the boresight error directly.

The current subroutine used to characterize the antenna permits selection of various polarizations and two aperture distributions. A uniform, circular aperture distribution having vertical, horizontal or

circular (LHR or RHC) polarizations is one combination. The second distribution is a tapered rectangular distribution having vertical polarization as found in flat plate antennas. This basic subroutine would not be difficult to modify to accommodate other distributions, such as rectangular aperture with cosine taper.

Computation time is independent of radome size but depends on the number of samples used in the aperture. For 256 sample points (16 X 16 array), the time to compute the received voltages in the three channels is 1.5 seconds.

The program is organized as a main program and a number of supporting subroutines, all written in Fortran IV. The complete program, including plotting software, contains thirty four subroutines. The core storage required for the complete program, including all library and system I/O routines, is just over 46,000 (decimal) words. Integer, real and complex variables and arrays are utilized. Single, double and three-dimensional data arrays are present. Only single precision variables and computations are required with the 60-bit word available on the Cyber 70 at Georgia Tech.

#### 1-4. References

1. E. B. Joy and G. K. Huddleston, "Radome Effects on Ground Mapping Radar", Contract DAAH01-72-C-0598, U. S. Army Missile Command, March 1973.
2. E. B. Joy, G. K. Huddleston, H. L. Bassett and C. L. Gorton, "Analysis and Evaluation of Radome Materials and Configurations for Advanced rf Seekers", Contract DAAH01-73-C-0769, December 1973.

3. E. B. Joy, G. K. Huddleston and H. L. Bassett, "Multi-Purpose Missile (MPM) High Performance Radome Trade-Off and Development Study", Martin Marietta Aerospace, April 1975.
4. G. K. Huddleston and E. B. Joy, "Development of Fabrication and Processing Techniques for Laser-Hardened Missile Radomes: Radome Electrical Design Analysis", Martin Marietta Aerospace, April 1977.
5. G. K. Huddleston, H. L. Bassett and J. N. Newton, "Parametric Investigation of Radome Analysis Methods", 1978 IEEE AP-S Symposium Digest, pp. 199-202, May 1978.
6. S. Silver, Microwave Antenna Theory and Design, New York, New York: McGraw-Hill Book Company, 1949.
7. D. T. Paris, "Computer-Aided Radome Analysis", IEEE Transactions, AP-18, no. 1, pp. 7-15, January 1970.
8. G. K. Huddleston, H. L. Bassett and J. N. Newton, "Parametric Investigation of Radome Analysis Methods", Annual Technical Report, AFOSR-77-3469, November 1978.
9. G. K. Huddleston, "Radome Analysis Computer Program: Surface Integration Formulation", Technical Report for Johns Hopkins University Applied Physics Laboratory, Contract 601053, February 1980.
10. G. K. Huddleston, H. L. Bassett, and J. M. Newton, "Parametric Investigation of Radome Analysis Methods: Comparisons of Analytical and Experimental Results", Scientific Report, Grant AFOSR-77-3469, in preparation.

Appendix C

Course Outline



PRE-REGISTRATION  
July 25 - 27, 1979

FALL QUARTER 1979

INSTRUCTOR: G. K. Huddleston

EE 8340 Radome Analysis

3-0-3. Prerequisites: Graduate standing, Maxwell's equations, antennas, vector analysis, and multivariable calculus.

Radome analysis is the application of basic electromagnetic theory to determine the effects of protective dielectric structures on the electrical characteristics of antennas so enclosed.

Course Objective: To enable the participants to derive selected important relations from Maxwell's equations and to apply them to the solution of practical electromagnetic problems dealing with the interaction of radiating structures and their dielectric enclosures; viz., radomes and electromagnetic windows.

Text: (1) S. Silver (ed.), Microwave Antenna Theory and Design, Volume 12 of MIT Radiation Laboratory Series (printed by Georgia Tech Bookstore)  
(2) Selected journal papers on reserve at library

Topical Outline

Definition of the Problem

History of radome development  
Electromagnetic windows  
Antenna systems  
Aerodynamic and mechanical considerations

Survey of Existing Analysis Methods

Geometrical optics (Silver)  
Equivalent aperture (Kilkoyne)  
Integral equation (Van Doeren)  
Equivalence and induction approach (Tricoles)  
Corrections for wall curvature (Tavis)  
Huygens principle (Paris)  
Plane Wave Spectrum (Wu and Rudduck)  
PWS and Equivalent Aperture (Joy and Huddleston)  
Spherical Wave Expansions (Chesnut)  
Lorentz reciprocity (Huddleston and Joy)

General Theory of Radome Analysis

Transmitting formulation  
Receiving formulation  
Integral equation  
Equivalence of formulations  
Electromagnetic windows

## Electromagnetic Theory

- Vector Green's theorem
- Kirchoff-Huygens principle
- Reciprocity theorem
- Equivalence theorems
- Geometrical optics
- Scattering
- Plane waves and infinite dielectric sheets
- Modal expansions for antenna radiation

## Special Considerations

- Coordinate systems and transformations
- Intersections of rays with surfaces of revolution
- Surface integration
- Approximations
- Comparisons of results

## Electromagnetic Windows

- Dielectric slab-covered waveguide
- Integral equation formulation
- Method of moments solution
- Radiation and impedance

## Boundary Value Problems

- Dipole within concentric spherical shell
- Spherical antenna with dielectric sheath
- Radiation from conical structures
- Ellipsoidal antenna with confocal dielectric sheath